The following supplement accompanies the article

Oceanographic, acoustic, and remote approaches reveal the spatio-temporal dynamics of blackfin snapper at an aggregation site in Palau

Megan Cimino*, Patrick Colin, Travis Schramek, Steven Lindfield, Michael Domeier, Eric Terrill

*Corresponding author: mcimino@ucsd.edu

Marine Ecology Progress Series 601: 185–201 (2018)

SUPPLEMENTAL INFORMATION

1. Acoustic Data Processing Methods

We processed the acoustic backscatter data in BioSonics' Visual Acquisition 6 and Visual Analyzer 4.3 software, similar to methods of Cimino et al. (2018). All analyses below were performed within these frequently utilized software programs produced by BioSonics Inc, which is a common approach used in other studies (ex. Bezerra-Neto et al. 2013, Kang et al. 2009, Farrell et al. 2017, Goodman et al. 2013, Langford 2012). Visual Acquisition was used to remove acoustic data collected when the REMUS traveled from east to west and was not detecting fish along the channel wall. Temperature and salinity recorded on the REMUS conductivity, temperature, and depth (CTD) sensor was used in post processing to calculate sound speed and absorption coefficients for each day, which was automatically done in the software. Using Visual Analyzer, bottom tracking was done manually to ensure that coral was not mistaken for fish. There was no acoustic dead zone near the channel wall. We limited our analysis from the channel wall to 0.5 m from the vehicle to remove sound intensity distortions due to the transducer near field effects. Using Visual Analyzer, the mean backscattering cross section and target strength for fish were estimated using the Expectation Maximization and Smoothing (EMS) method (Hedgepeth 1994, Hedgpeth et al. 1999), a robust iterative statistical technique for single-beam data. The EMS method is based on the distribution of targets versus target strengths and the probability of placement within the acoustic beam. For completion of the EMS procedure, a minimum echo count of 200 was required per survey day (recommended Visual Analyzer setting). The EMS procedure is outlined in detail in BioSonics (2011). The EMS method is a part of the echo integration calculation. Echo integration was used to estimate the number of acoustics targets, which allows the measured energy return for a given volume of water to be used to estimate target populations. In Visual Analyzer, the echo integration method uses the above target strength estimation technique to find a mean backscattering cross section value to estimate fish density (Biosonics 2011). The average energy contained in a given volume of water is scaled by environmental/calibration parameters, providing an estimate of volume backscattering strength. The target strength range was set to -25 to -55 dB, which removed background noise and other weak unwanted echoes. This wide target strength range was appropriate given echogram visualizations and may be due to variations in body orientation when fish are viewed horizontally (likely resulting in anterior, posterior, or lateral views), compared to standard methods of upward/downward looking echosounders in which fish body orientation is likely more consistent (ventral or dorsal view). Other echo recognition parameters included a correlation factor of 0.9, minimum and maximum pulse width factor of 0.75 and 2, and end

point criteria of -6 dB. Using Visual Analyzer, the measurements were binned into 1 m bins from the vehicle to the channel wall and into 5 m bins along the vehicle track. Fish per cubic meter is the estimate of the number of fish in a volume of water; it is the sum of the volume backscatter strength divided by the backscattering cross section. Values for fish per cubic meter were outputted for each 1 by 5 m grid cell along the REMUS track. Fish per unit area (or m^{-2}) estimates the number of fish in the water column; it is the sum of the absolute density times the interval thickness times the proportion of the interval sampled. Values for fish m^{-2} were outputted every 5 m along the REMUS track.

The echosounder was calibrated by BioSonics Inc. using a reference-standard transducer in their hydroacoustic calibration facility in 2008. We recognize this was three years prior to our first survey and unfortunately, no calibrations were made in the field. In 2016, we calibrated the echosounder using the standard (tungsten carbide) sphere method (Foote et al. 1987) and following procedures recommended by the producer (BioSonics, Inc). We found a small -2.5 dB offset. This suggests there was likely little to no offset during the time of our surveys in 2011 and 2012. However, this should be taken into consideration when interpreting our results of average target strength reported for single targets.

Fish can often be identified to species using a target strength range known for a given species and the accurate conversion from echo integration to animal densities depends on these estimates of individual target strength (Simmonds and MacLennan 2005). However, acoustic backscatter from a fish is complex with echo intensity resulting from multiple factors including fish size, fish orientation, swim bladder characteristics and acoustic frequency. We were not able to identify a species solely based on acoustic return because specific target strength ranges for *L. fulvus* measured horizontally and pinged by 200 kHz transducer are unknown. Some other species of similar size, potentially acoustically indistinguishable from *L. fulvus,* had small schools of individuals in our study area including, *Gnathodentex aurolineatus* (a resident), *Pterocaesio tile*, *Plectorhinchus chrysotaenia* and a potential spawning aggregation of *L. gibbus*. However, when the full *L. fulvus* aggregation was present, its numbers far exceeded all other fishes combined (visual observations while diving/snorkeling and time-lapse photos). All echograms were visually examined to confirm all targets of interest were counted. In addition, we compared the acoustic detection of fish aggregations with time-lapse photos taken at the same time, which confirmed that all acoustically detected fish at camera locations were almost exclusively *L. fulvus*.

2. Results on Fish Detected Only in Early November

Twelve of the twenty fish tagged were only detected during early November (Fig. S4), near the time of their tagging. These fish were 22 to 24.5 cm total length, both male and female (Table S2), and their lengths not significantly different than fish detected in more than one month (t-test $t = 0.19$, $df = 10.19$, $p = 0.85$). Eight of these fish were present within the aggregation site during the day of their release but left around the time of sunset and were never detected again. Two of the fish (17, 19) left the aggregation site on the fifth day after the full moon and were never detected again. Fish 16 was present at receiver D and was the only fish to move far to the east to receiver J and was never detected again. It is possible that this fish was consumed and therefore, this uncharacteristic movement was in reality a larger predator. Atypically, fish 14 made larger movements, swimming from the aggregation site to receiver I on the southeast edge of the channel (the only fish detected here), then swam through the aggregation site to receivers G and H on the northwest edge of the channel and was last detected at the aggregation site. Fish 13 left the aggregation site and was the only fish detected on receiver F located on the northeast end of the channel. These fish that were only detected during early November displayed more variable behavior, with some staying at the aggregation site longer than the full moon period or visiting locations that fish with more consistent behavior did not (Fig. 2). Mortality from tagging or predation may account for lack

of detection in subsequent months. During this time period in early November 2012, >90% of the detections were within the aggregation site with 11%, 25%, 7%, 46% and 4% of the detections at receivers A-E, respectively (Fig. S4).

3. Detailed Individual Fish Movements between the Channel Mouth and Aggregation Site

Three fish were detected ten times on receiver G and H (Fig. 2a), near the channel mouth, from late November to January between sunset and midnight. We will discuss each of the three fishes movements separately (Table 2). First, on four separate days, twice during two separate full moon periods, fish 5 (male) left the aggregation site around sunset (sunset at ~17:50) and was detected at receiver G/H ~40 min later (range 35 to 70 min). After the four trips to the channel mouth, this fish was next detected at the aggregation site the following morning after sunrise on two occasions, at the aggregation site the same night ~3 h later on one occasion and not detected again that full moon period on the final occasion (Table 2). Second, fish 6 (male) left the aggregation site before sunset on December 30 (sunset at 17:55), was detected at receiver G at 21:00, and was next detected the following morning at 8:16 within the aggregation area. Third, on three separate days, during two full moon periods, fish 7 (female) was detected five times at receiver G/H. On two of these days, fish 7 was detected on G/ H twice in one night with a 1 and 8 min interval between detection times. Fish 7 was predictably detected at receiver G/H at ~21:00, and returned to the aggregation site on one occasion 10 min later and on another 48 min later. Its minimal travel time recorded between the aggregation site and receiver G/H was 10 minutes, suggesting the fish swam ~500 m at 0.8 m/s, a realistic speed for this size fish.

Fish detected at the channel mouth had similar movement patterns. These fish appeared to be making repeated movements towards the channel mouth (receiver G/H) around the time of the highest tide of the day, which was at ~19:40 in November, ~20:20 in December and ~21:00 in January (Table 2). Fish 5 was detected on receiver G/H between 40 min to 2 h before high tide at nearly the same time each night (~19:00). Fish 6 was detected 40 min after high tide, and fish 7 was detected less than 30 min after high tide at nearly the same time each night (~21:00). Many fish could be aggregating or swimming together within the vicinity of receiver G/H as fish 6 and 7 were detected on receiver G at approximately the same time (~21:00) on December 30 (Table 2). When fish were detected back at the aggregation site, it was always after high tide. There was no apparent pattern to the previous or next receiver that fish were detected on before or after being detected at G/H. However, the fish were most frequently detected on middle receivers B, C and D (never A), suggesting fish do not transit along the channel wall at shallow depths otherwise fish would have been detected on receiver A.

4. Dye Study Results

To further map the flow near the aggregation site and understand the resulting transport pattern, uranine dye was released during a falling tide near the site and we made visual observations (Fig. S10 C-F) and recorded information (Fig. S11) on the dye as it flowed out of the channel. The first release of dye was made at 12:32 (just after high tide at 12:06) upstream of the eddy-like feature from the channel side to ~55 m off the wall (Fig S11a). We expected that the dye would become entrained within the eddy; however, this was not the case. Instead, the dye in surface waters quickly flowed towards the middle of the channel, then outwards towards the channel mouth without entering the eddy (Fig. S10 & S11). A similar trajectory was seen with both drogues that were released at a similar time, where one was released near the channel wall and the other closer to the middle of the channel. The dye was highly concentrated (>144 ppb) at 12:42 (Fig. S10c) but had a larger footprint and lower concentration (~40 ppb) at 13:10 (Fig. S11a). During the second dye study, approximately one hour later, a lower quantity of dye was released within the northwest corner of the eddy-

like feature (Fig. S11b). The dye was also quickly transported out of the channel mouth as were the drogues that were released at a similar location. Notably, drogue 1 drifted counter-clockwise from the release location towards the channel wall and back to the release location (Fig. S12) before being transported towards the middle of the channel and then out the channel mouth (Fig. S10). The drogue drifted at a speed of 0.25 to 0.6 m/s within the feature and <0.4 m/s as it was transported towards the middle of the channel. The dye release provided useful information on flow during the outgoing tide. The average and maximum speed of drogues were ~0.5 and ~0.7 m/s (Table S3), with speeds increasing from the channel wall towards and out of the channel mouth. These drogue current velocities are comparable to HADCP measurements, which showed mean velocities of 0.24 and 0.87 m/s near the channel wall and in the middle of the channel (Fig. S9).

SUPPLEMENTAL REFERENCES

BioSonics, Inc. (2011) User Guide, Visual Analyzer 4. Seattle, WA, pp 54-58.

Bezerra-Neto JF, Brighenti LS, Pinto-Coelho RM (2013) Implementation of hydroacoustic for a rapid assessment of fish spatial distribution at a Brazilian Lake-Lagoa Santa, MG. Acta Limnologica Brasiliensia 25(1):91-8

Cimino M, Patris P, Ucharm G, Bell L, Terrill E. 2018. Jellyfish distribution and abundance in relation to the physical habitat of Jellyfish Lake, Palau. J Trop Ecol 34(1): 17-31.

Farrell JL, Siegfried CA, Daniels RA, Sutherland JW, Boylen CW, Bloomfield JA, Quinn SO, Nierzwicki-Bauer SA (2017). The dynamics of *Chaoborus americanus* in an Adirondack lake following the reintroduction of fish. Limnologica 65:38-45.

Foote KH, Knudsen G,. Vestnes DN, Maclennan, Simmonds EJ. 1987. Calibration of acoustic instruments for fish density estimation: A practical guide. ICES Coop Res Rep 144:69

Goodman SE, June JA, Antonelis KL, Antonelis AL. (2013) Acoustic Survey of Fishes in the Chukchi Sea Environmental Studies Program in 2012.

Hedgepeth JB (1994) Stock Assessment Via Tuning and Smoothed EM Estimation. PhD dissertation, University of Washington, WA.

Hedgepeth JB, Gallucci VF, O'Sullivan F, and Thorne RE. 1999. An expectation maximization

and smoothing approach for indirect acoustic estimation of fish size and density. ICES J Mar Sci 56: 36–50.

Kang D, Cho S, Lee C, Myoung JG, Na J. (2009) Ex situ target-strength measurements of Japanese anchovy (*Engraulis japonicus*) in the coastal Northwest Pacific. ICES J Mar Sci 66(6):1219-24

Langford B. 2012. Analysis of the Fish Community on Tidal-Freshwater Constructed Reefs. Master's thesis. Virginia Commonwealth University, VA.

Simmonds J, MacLennan DN (2005) Fisheries acoustics, theory and practice. 2nd ed., Blackwell Science, Oxford, p 456.

SUPPLEMENTAL TABLE

Supplemental Table 1. An overview of our methods, the dates the methods were employed and the rationale for using each approach. A detailed description of each method can be found in the methods section.

Method	Dates	Rationale
Bathymetry 1) Airborne LIDAR 2) Single point sonar 3) Multi-beam/Echoscope sonar	1) 2004 2) 2009 3) 2012	Create detailed bathymetry maps to examine effects of topography on current patterns and fish aggregation locations.
Acoustic Telemetry 1) Tag fish 2) Deploy receiver array	1) October 31, 2012 2) April 2012 - October 2013	Implant acoustic tags within fish and deploy an array of acoustic receivers to track fish spatial and temporal movements across hours to multiple months
Underwater Time-lapse Cameras	March 19-24, 2011; March 5-15, 2012	Document the presence/absence and movements (via fish body orientation) of fish at the aggregation site during two spawning periods during daylight hours
Above water Time-lapse Camera	March 10, 2012	Document an eddy-like feature that is visible on the sea surface; a possible aggregation cue.
Horizontal-ADCP	March 5-12, 2012	Measure current velocities across West Channel, which may influence fish distributions
Thermographs	January 8- May 15, 2012 July 5-12, 2010	Measure temperature in West Channel across seasons and depths; a known factor that influences fish behavior
REMUS AUV with integrated echosounder, CTD, ADCP	March 21, 2011 March 8-10, 2012	Map the distribution and abundance of fish, and water properties along the channel wall at different depths during the aggregation period
Dye Experiment with Drogues	January 19, 2017	Understand current flow within an eddy-like feature at the aggregation site and in West Channel. Provide spatial data to compare with stationary horizontal-ADCP.

Abbreviations: Light Detection and Ranging (LIDAR), acoustic Doppler current profiler (ADCP), autonomous underwater vehicle (AUV), conductivity-temperature-depth (CTD).

Supplemental Table 2. Length and sex of blackfin snappers that had a surgically implanted acoustic tag. For sex, F=female, M=male, U=unknown.

Tag ID	Standard Length (cm)	Total Length (cm)	Sex
1	21.0	24.5	F
2	21.5	25.5	F
3	19.0	22.5	M
4	20.0	23.5	M
5	19.5	23.0	M
6	18.5	22.0	M
7	21.5	25.0	F
8	20.0	23.5	M
9	20.0	23.5	F
10	20.0	23.5	F
11	20.0	23.5	F
12	21.0	24.5	U
14	19.0	22.0	M
14	19.0	22.5	U
15	20.5	24.0	M
16	20.5	24.0	F
17	20.0	23.5	M
18	19.5	22.5	U
19	21.0	24.5	F
20	20.0	23.0	M

Supplemental Table 3. The average speed and total distance that each drogue traveled during the dye experiment 1 (Fig. S11a) and 2 (Fig. S11b). Orange and red corresponds to colored drogue trajectories in Fig. S11.

Dye Experiment	Drogue [color]	Total Distance (m)	Average [Maximum] Speed (m/s)
1	1 [orange]	431.35	0.50 [0.65]
1	2 [red]	430.82	0.52 [0.67]
2	1 [orange]	1274.09	0.53 [0.76]
2	2 [red]	922.64	0.50 [0.80]

SUPPLEMENTAL FIGURES

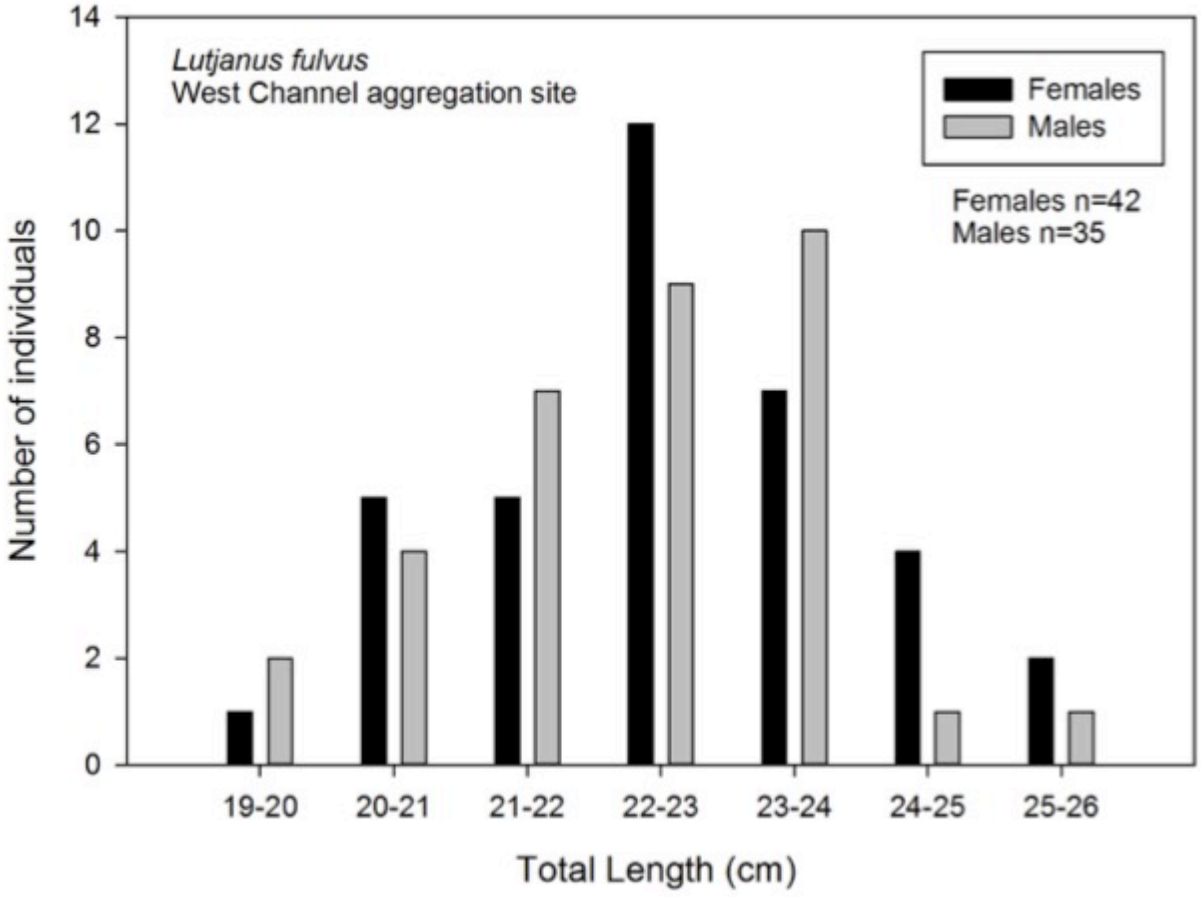

Supplemental Figure 1. Size frequency for total length of *Lutjanus fulvus* captured at the West Channel aggregation site since 2004 (including data from Sadovy de Mitcheson et al. 2012). Data is binned by 2 cm. The size frequency structure is consistent with a normal fish population without any fishery pressure.

Supplemental Figure 2. Examples of GoPro time-lapse photographs taken at camera 1 at the aggregation site. (a) A large number of fish present near the camera, (b) a large number of fish but distant from camera and (c) no fish present near the camera. The local time and date of each photo is included.

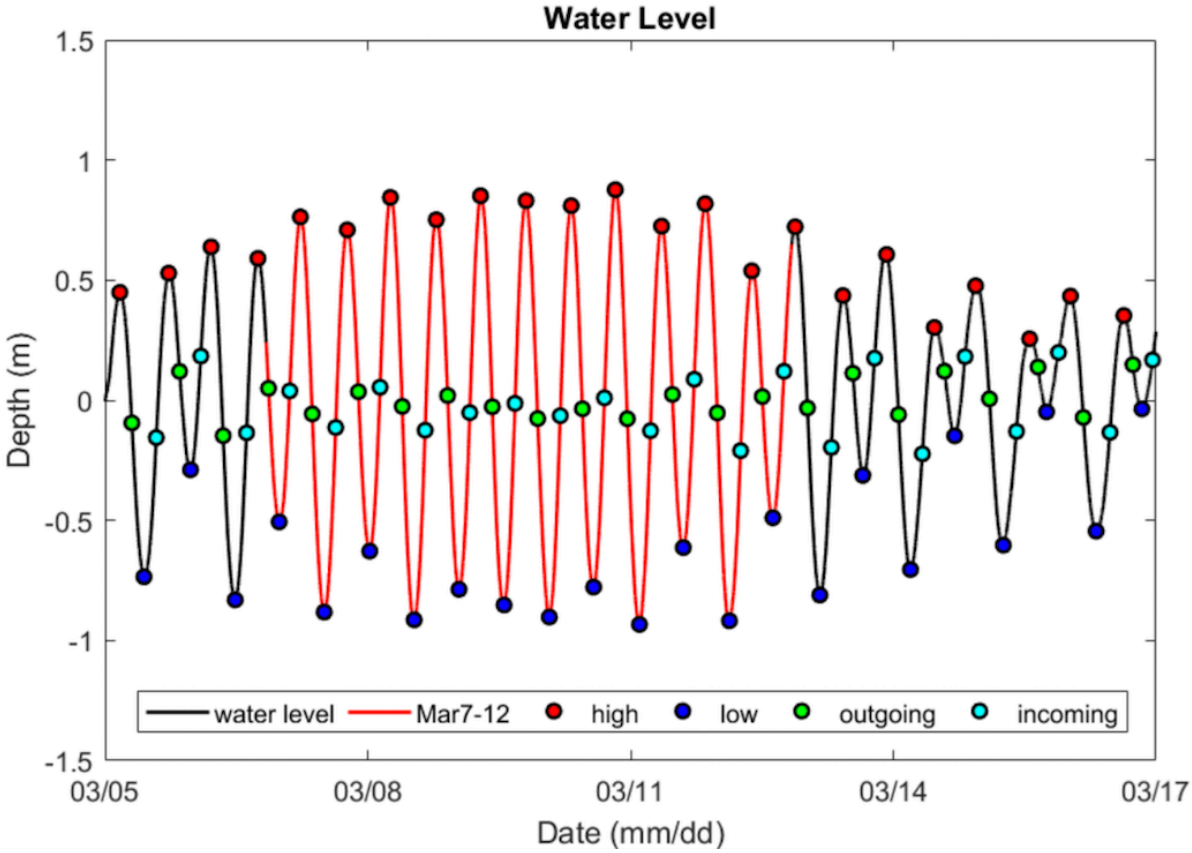

Supplemental Figure 3. De-tided water level measured at the horizontal ADCP. The time period during the presence of the aggregation is in red. High, low, outgoing and incoming tide is shown (used in Fig. 6 to separate tide phases).

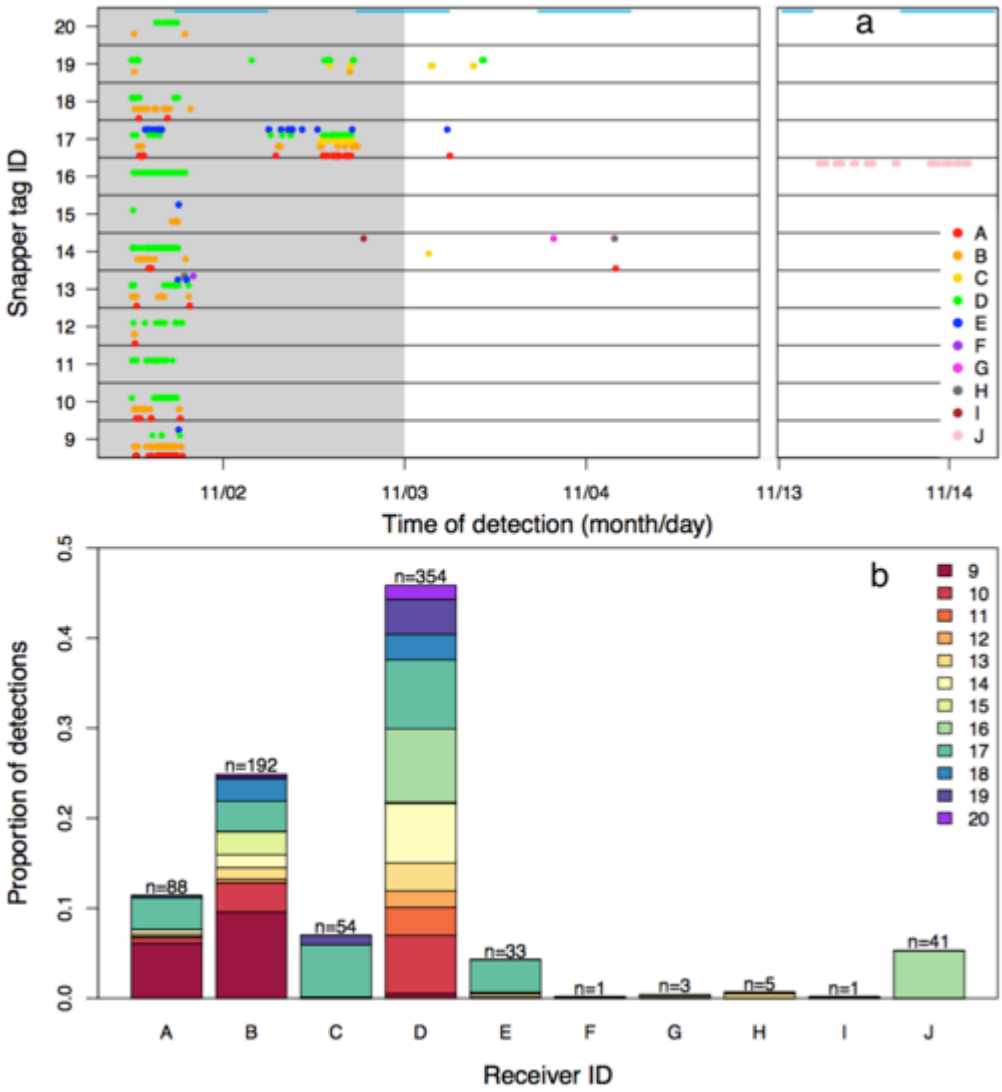

Supplemental Figure 4. The presence and absence of telemetered blackfin snapper that were only detected in early November 2012 at VEMCO acoustic receivers. (a) Time of acoustic detections for each fish at different receivers (A-J). Gray shading indicates the time of the full moon until four days after. The color of the receiver matches receiver locations in Fig. 1a. Horizontal blue lines are the time between sunset and sunrise. (b) The proportion of snapper detections on each acoustic receiver. The colors correspond to snapper tag ID. Sample size (n) is the number of detections at each receiver

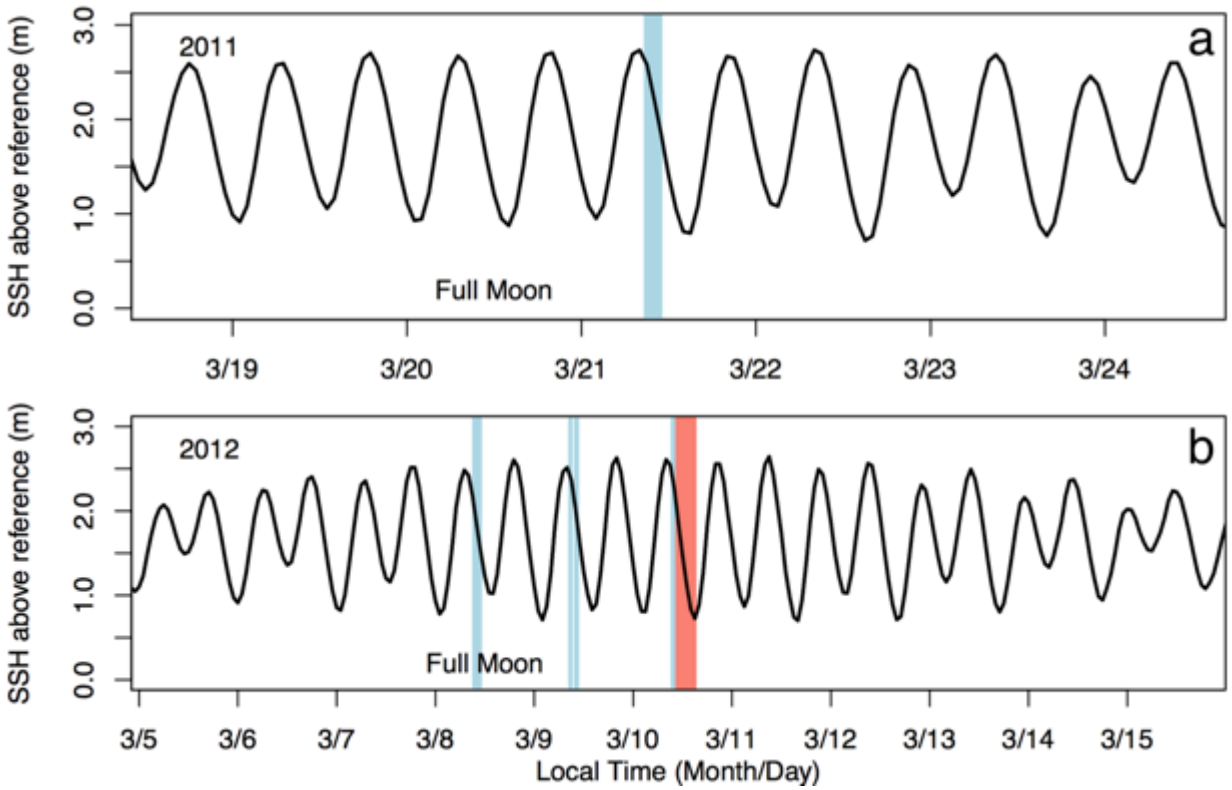

Supplemental Figure 5. Sea surface height (SSH) during the duration of the fish time-lapse camera deployment (#1-4, Fig. 1b) in March (a) 2011 and (b) 2012. REMUS missions are highlighted in blue, the sea surface time-lapse is in red and the date of the full moon is shown.

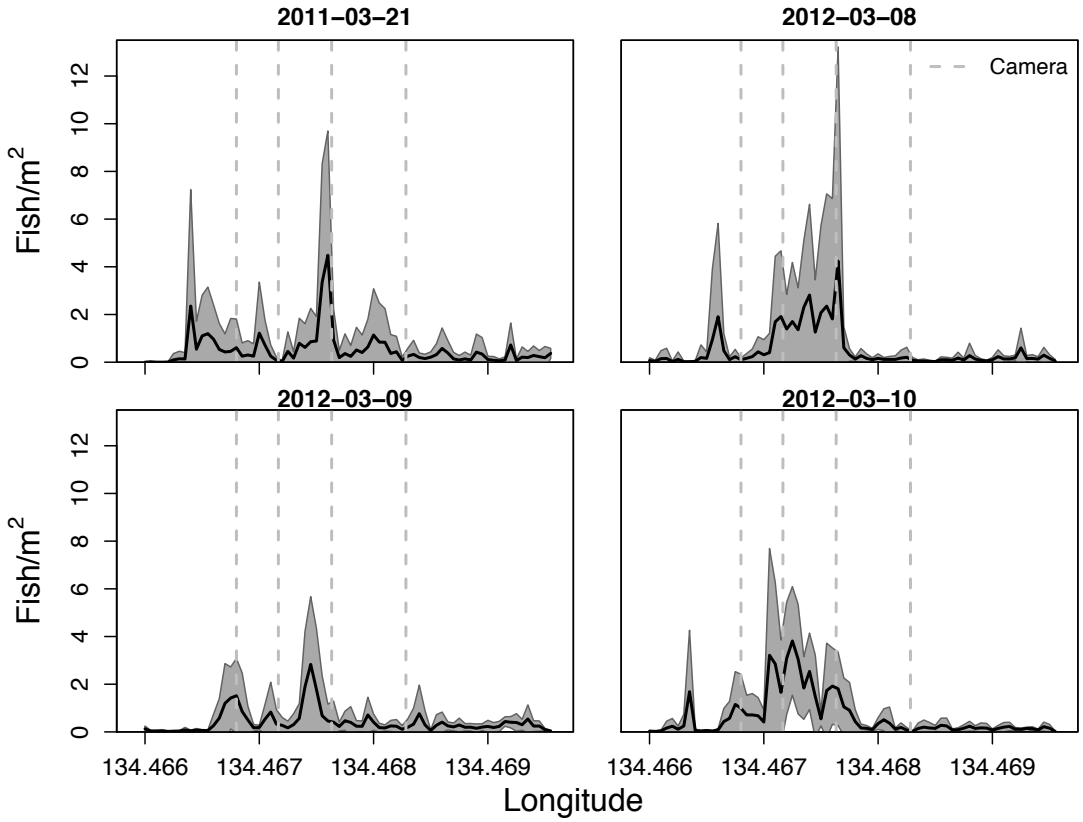

Supplemental Figure 6. Average fish density across all depths along the REMUS mission track. The mean and standard deviation in fish m^{-2} on (a) March 21, 2011, (b) March 8, 2012, (c) March 9, 2012, (d) March 10, 2012. Vertical gray lines represent time-lapse camera locations (from left to right is Camera 4 to 1).

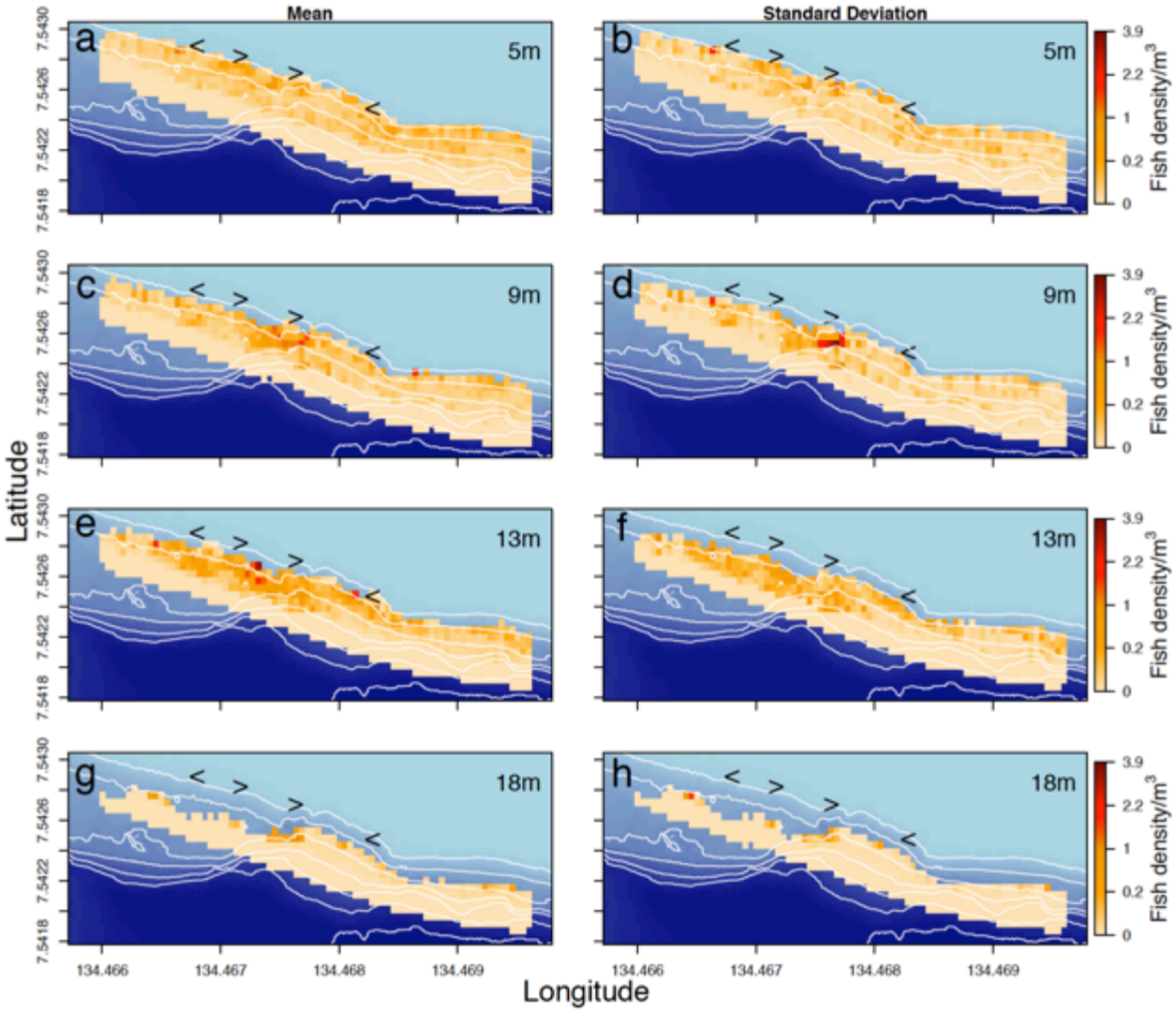

Supplemental Figure 7. The spatial distribution of fish density at each survey depth. The mean (a,c,e,g) and standard deviation (b,d,f,h) in the maximum fish density m^{-3} for each depth: 5m (a,b), 9m (c,d), 13m (e,f) and18m (g,h). For each survey, the maximum density within each 5 m^2 grid cell was computed and then the average and standard deviation of the maximums were taken for all surveys at each depth for all years. There was only one survey at 18 m and the mean for this transect is shown. Black arrows represent locations of time-lapse cameras.

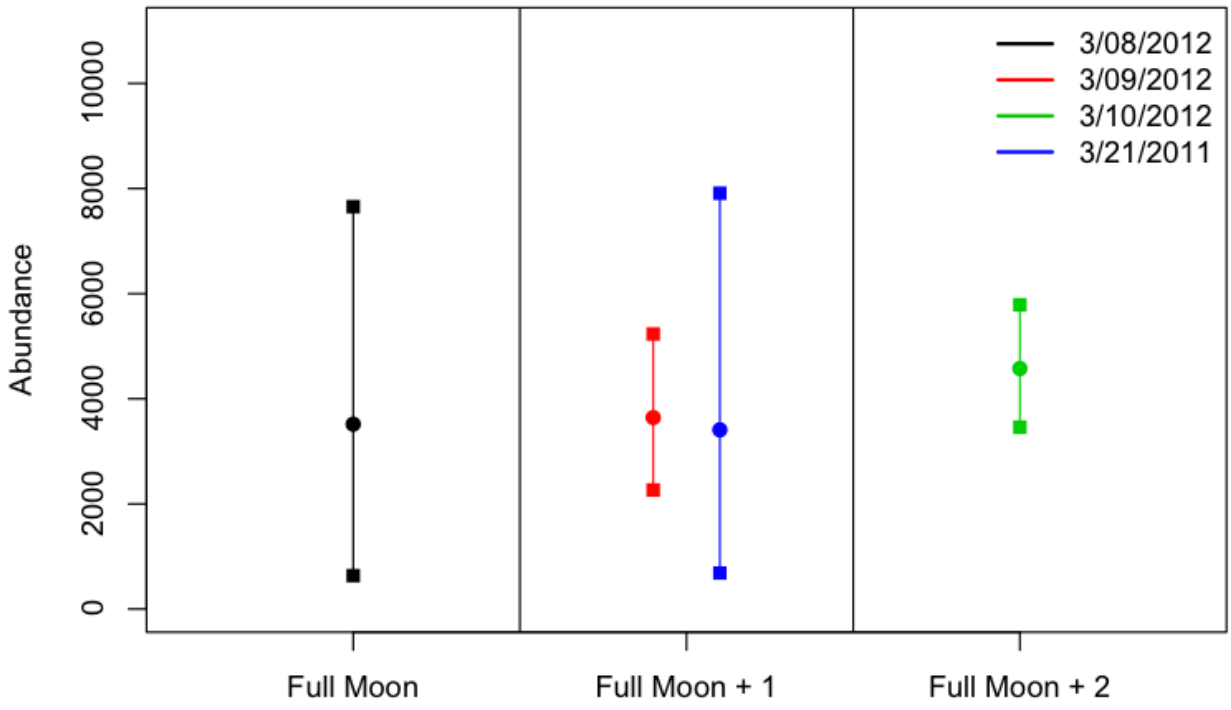

Supplemental Figure 8. *L. fulvus* total abundance estimates for each REMUS survey day in relation to the full moon. The circle is the sum of the interpolated mean abundance per grid cell across all depth layers while the squares represent the sum of minimum/maximum abundances.

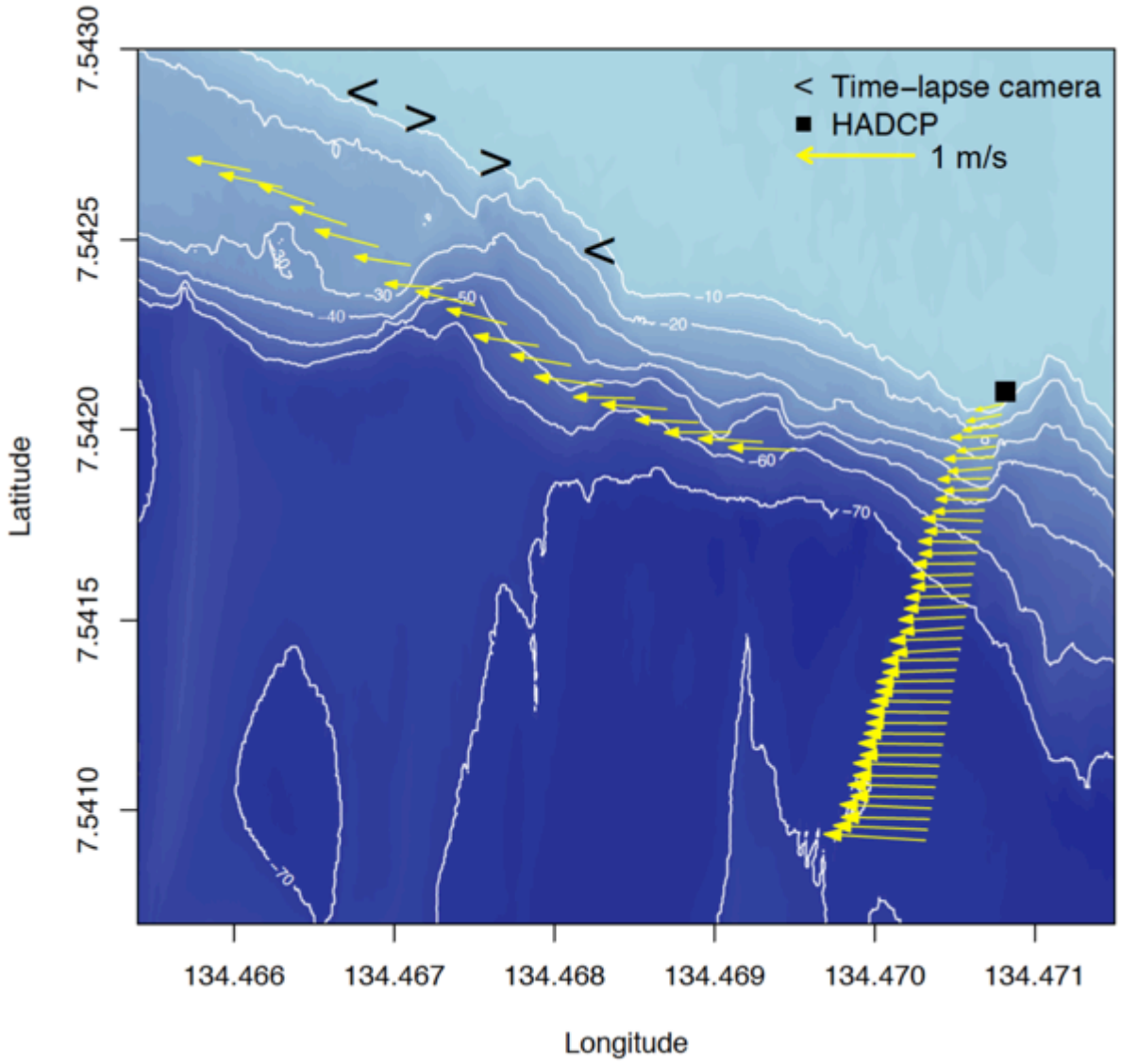

Supplemental Figure 9. Comparison of mean currents from the ADCP on the REMUS and the HADCP on the outgoing tide. The location of time-lapse cameras are shown for reference.

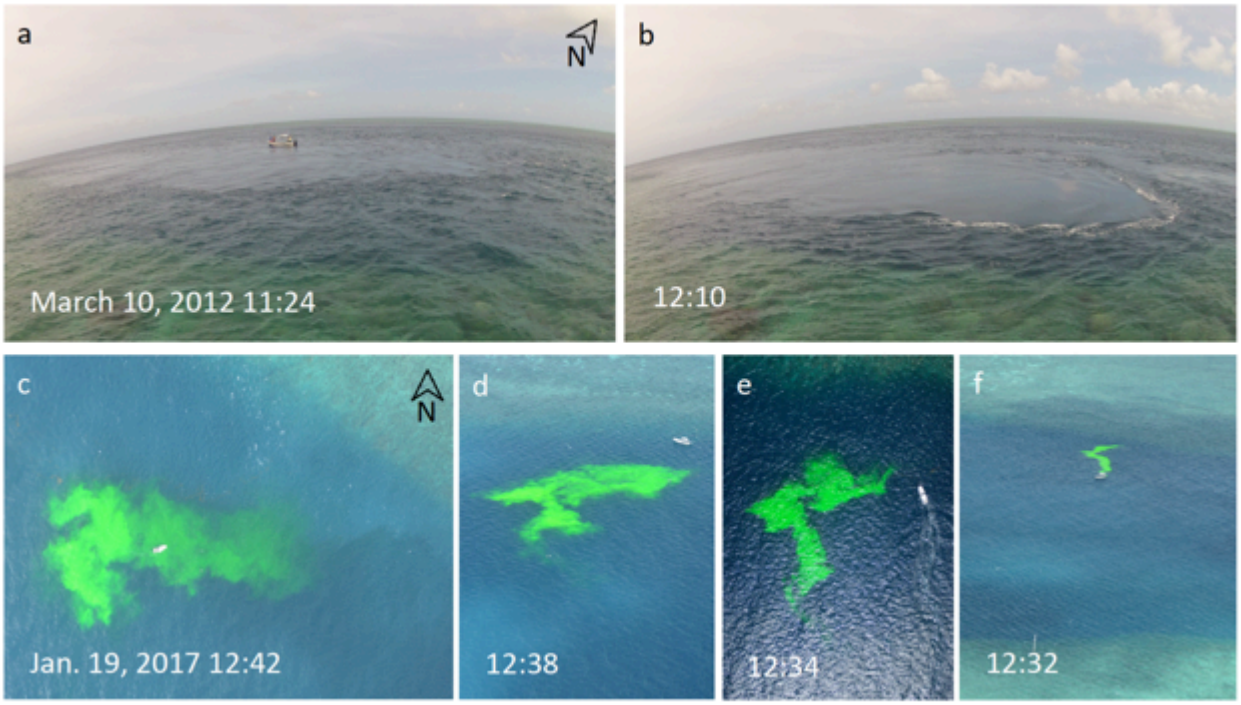

Supplemental Figure 10. Photographs of an eddy-like feature and the dye trace during the first release. (a,b) Two examples of the eddy-like feature that occurred on the outgoing tide from the sea surface time-lapse camera (Fig. 1b). A similar eddy-like feature on the scale of ~100 m occurs during the outgoing tide at the fish aggregations site. (c,d,e,f) West to east imagery of the dye evolution taken from a plane at ~500 ft (Photo credit: P. Colin). Local time and date is shown on the photos and can be matched to Fig. S11 for spatial orientation. For scale, a 150 HP Yamaha boat (8 m) is pictured.

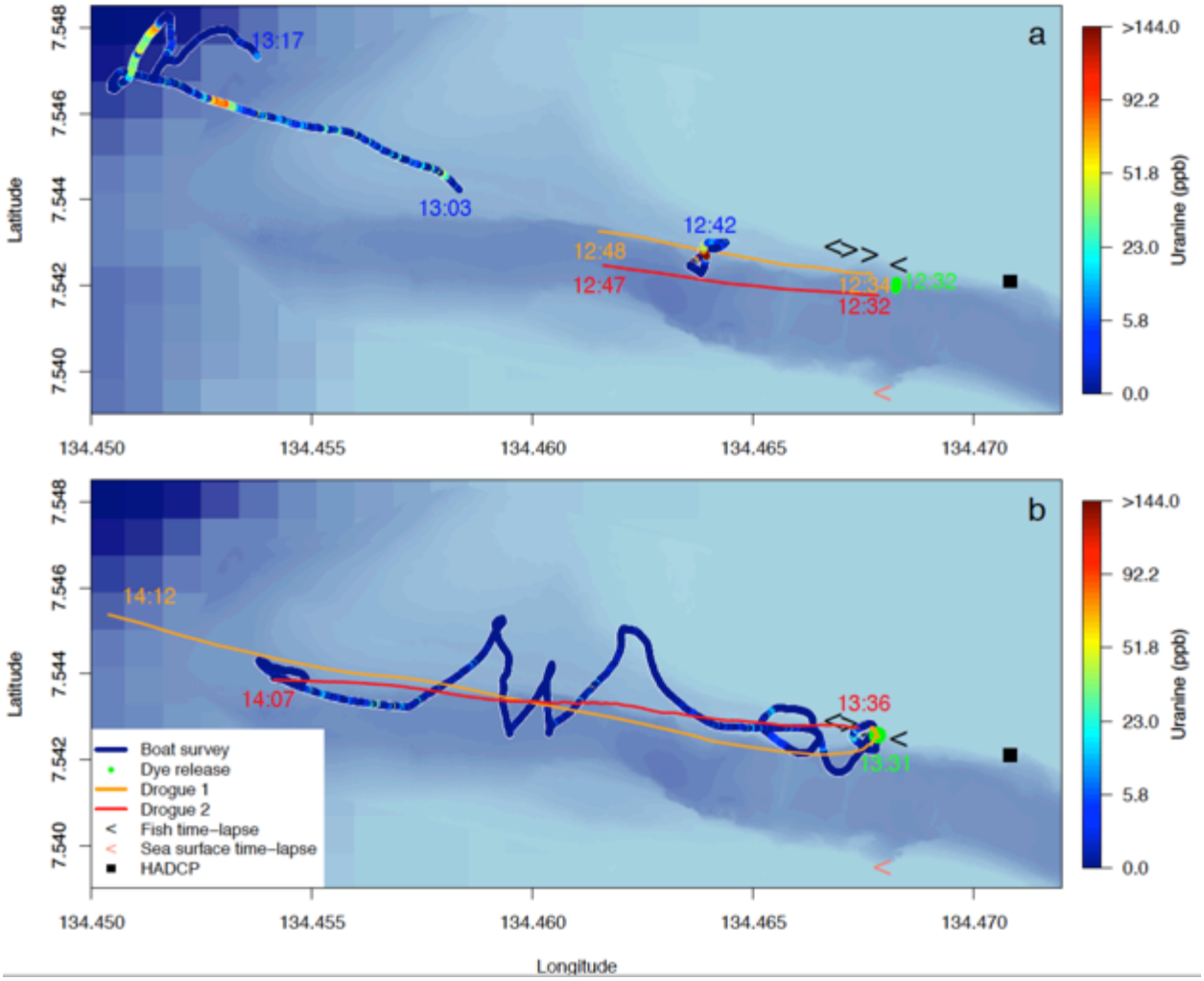

Supplemental Figure 11. Uranine dye and two surface drogues were released near the fish aggregation site in West Channel to study ocean currents on the outgoing tide of January 19, 2017. The dye and drogues were followed in a small boat that measured uranine concentrations. (a) At 12:32, dye was released in a straight line upstream of the aggregation site (Fig. S10F). (b) At 13:31, a smaller quantity of dye was released in the middle of the fish aggregation site within the eddy-like feature. The locations of other instruments are shown for spatial reference. High tide was at 12:06 (5.2ft).

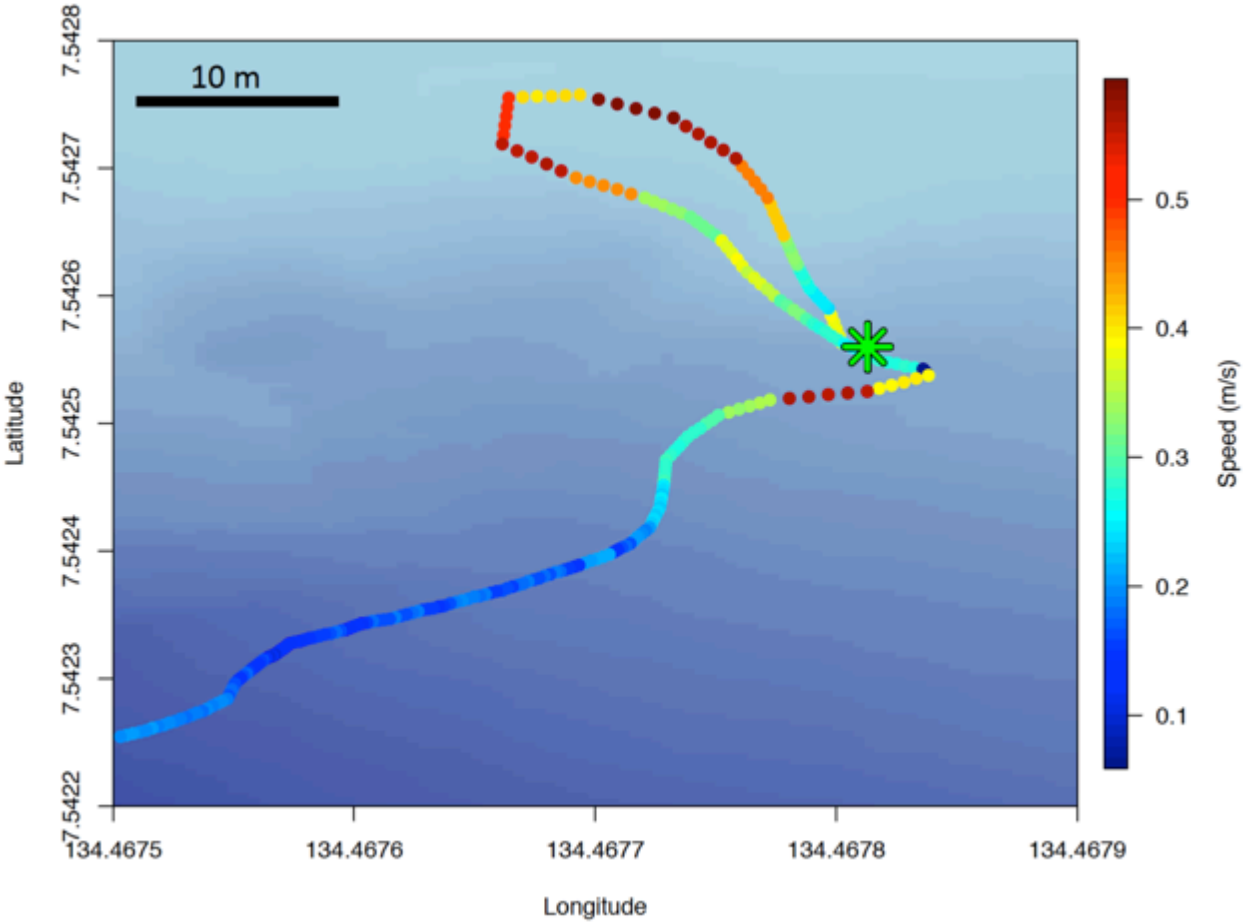

Supplemental Figure 12. Speed of drogue 1 (orange) in dye experiment two (Fig. S11b) near the dye release location (green star). The drogue made a counterclockwise loop before drifting offshore, perhaps evidence that it was entrained in an eddy-like feature for a short period of time.